

## Numerical simulation of bubble-train flow with heat transfer in a square mini-channel

Bradut Eugen Ghidersa<sup>1</sup>, Martin Wörner<sup>2</sup>, Dan Gabriel Cacuci<sup>3</sup>

1: Forschungszentrum Karlsruhe, Institut für Reaktorsicherheit, Germany, ghidersa@irs.fzk.de

2: Forschungszentrum Karlsruhe, Institut für Reaktorsicherheit, Germany, woerner@irs.fzk.de

3: Forschungszentrum Karlsruhe, Institut für Reaktorsicherheit, Germany, cacuci@irs.fzk.de

---

**Abstract** To model convective heat transfer for a spatially periodic two-phase flow in a channel with large length-to-hydraulic diameter ratio, a new concept, called *periodic fully developed flow and heat transfer*, is proposed. After a few hydraulic diameter away from the channel inlet the flow characteristics are free from entrance effects. For this region, the identification of the periodicity characteristics of the flow enables to reduce the analysis of the flow field and temperature distribution to a single isolated module. Using this method the flow of a train of large bubbles uniformly distributed along a 2 mm wide channel with square cross-section is simulated. The convective heat transfer inside the channel due to a uniform wall heat flux is considered and the modification of the temperature field due to the presence of the bubble is analyzed.

---

### 1 Introduction

Microfabrication techniques developed within last decades made possible the building of miniaturized devices with high mixing and favorable heat transfer characteristics (Ehrfeld et al., 2000; Schubert et al., 2001). Consisting of large number of nominally identical flow channels with hydraulic diameter of order of 1 mm or smaller, these devices are increasingly used in different fields of chemistry due to their capabilities that are exceeding those of conventional macroscopic systems (Jensen, 2001). Compact heat exchangers with enhanced heat transfer rates and micro-reactors with increased specific interfacial areas, compared with classical devices, are only two examples of industrial applications, where such kind of systems are intended to replace the existing technologies in order to increase the efficiency. In many of these applications frequently gas-liquid two-phase flow occurs. Because the importance of surface tension increases with decreasing channel size the hydrodynamics of gas-liquid two-phase flow in small channels in principal differ from that in a macro-channel with direct impact on the heat transfer characteristics of the flow. For design, optimization and safe operation of devices built from micro-channels the understanding of the basic phenomena in a single channel is mandatory.

Our goal here is to define a method that enables the direct numerical simulation (DNS) of 3D gas-liquid flows in rectangular mini-channels when heat transfer is considered. The direct numerical simulations are performed with an extended version of our in-house computer code TURBIT-VOF, which was originally developed for investigation of bubbly flow in large channels (Sabisch et al., 2001). The code is based on a volume-averaged set of equations for the entire domain, which expresses the conservation of mass, momentum and enthalpy (Ghidersa, 2003). To account for the phase-interface evolution the volume fraction of the continuous phase is tracked using a Volume of Fluid method.

Small channels are characterized by large length-to-hydraulic diameter ratio, therefore, after a few hydraulic diameters away from the channel inlet, the flow characteristics are free from entrance effects. For this region, the identification of the periodicity characteristics of the flow enables to reduce the analysis of the velocity field to a single isolated module and use of periodic boundary conditions to take in account the influence of the upstream and downstream flow (Ghidersa et al., 2004). In contradistinction, the temperature distribution is not independent of the stream-wise coordinate even if the flow is fully developed. However, when the heating of the channel is done by a uniform wall

heat flux, the temperature could be decomposed in a linear variation along the channel and a reduced temperature field characterizing the local distribution in the module. This method has been already used successfully by Patankar et al. (1977) to model heat transfer for single phase flows in ducts with stream-wise-periodic variations of the cross-sectional area. In section 2 this procedure is extended to model periodic two-phase flows and a new concept, called *periodic fully developed flow and heat transfer*, will be introduced. As typical example of periodic gas-liquid two-phase flow, the slug flow in small channels is considered. In section 3 the flow of a train of large bubbles uniformly distributed along a 2 mm wide channel with square cross-section will be simulated. The convective heat transfer inside the channel due to a uniform, both axially and perimetrically, wall heat flux will be analyzed. Finally, section 4 presents a summary and the conclusions.

## 2 Convective heat transfer for a spatially periodic two-phase flow

We consider the case of a slug flow of two incompressible fluids in a straight rectangular mini-channel. The flow consists of a regular (periodic) train of bubbles which occupy most of the channel cross-section and are often denoted as Taylor bubbles. The individual bubbles are separated by liquid slugs which are, in narrow channels, free of smaller bubbles. This type of flow is also referred as bubble-train (BT) flow (Thulasidas et al. , 1995).

Let us consider the case when the channel is heated/cooled by an axially uniform wall heat flux ( $q$ ). Since the flow is periodic with a periodicity length  $L$  it means that the temperature profiles for  $y$ ,  $y + L$ , ... have the same slope at the wall<sup>1</sup>. Thus, in the case of the periodic thermally developed regime the temperature profiles at the stream-wise positions  $y$ ,  $(y + L)$ ,  $(y + 2L)$ , ... will have identical shape and, for the case of heating, will be displaced one above the other by the same distance:

$$T_{\varphi}(x, y + L, z) - T_{\varphi}(x, y, z) = T_{\varphi}(x, y + 2L, z) - T_{\varphi}(x, y + L, z) = \dots \quad \varphi = 1, 2 \quad (1)$$

Further, for each phase  $\varphi$ , let us define:

$$\theta_{\varphi}(x, y, z) = \frac{T_{\varphi}(x, y + L, z) - T_{\varphi}(x, y, z)}{L} \quad \varphi = 1, 2 \quad (2)$$

and subdivide the temperature field in two components:

$$T_{\varphi}(x, y, z; t) = y\theta_{\varphi}(x, y, z; t) + \Theta_{\varphi}(x, y, z; t) \quad \varphi = 1, 2 \quad (3)$$

Further on we will refer to  $\theta$  as linear temperature coefficient and to  $\Theta$  as the reduced temperature field<sup>2</sup>. For now,  $\theta$  is assumed to vary both spatially and in time, and it is defined separately for each fluid  $\varphi$ .

The periodic fully developed heat transfer condition (1) implies that  $\theta_{\varphi}$  is periodic in stream-wise direction ( $y$ ), that is:

$$\theta_{\varphi}(x, y, z; t) = \theta_{\varphi}(x, y + L, z; t) = \theta_{\varphi}(x, y + 2L, z; t) = \dots \quad \varphi = 1, 2 \quad (4)$$

as well as the reduced temperature  $\Theta_{\varphi}$ :

$$\Theta_{\varphi}(x, y, z; t) = \Theta_{\varphi}(x, y + L, z; t) = \Theta_{\varphi}(x, y + 2L, z; t) = \dots \quad \varphi = 1, 2 \quad (5)$$

This means that, in case of heat transfer problems subject to (1) the temperature field can be described using two periodic fields, one that takes in account the overall temperature variation along the channel ( $\theta$ ) and the other ( $\Theta$ ) giving the temperature distribution due to the local heating.

<sup>1</sup>In this paper the channel is assumed to be parallel with  $y$ -axis with walls at  $x = 0$ ,  $x = 1$  and  $z = 1$ ,  $z = 2$ .

<sup>2</sup>The term "reduced" refers to the fact that, inside each module of length  $L$  the temperature  $\theta$  has the same spatial distribution.

For each fluid  $\varphi$ , in the bulk region, the heat transfer and convection is governed by the local enthalpy equation:

$$\frac{\partial \rho_\varphi C_{p,\varphi} T_\varphi}{\partial t} + \nabla \cdot (\rho_\varphi C_{p,\varphi} T_\varphi \vec{v}_\varphi) = \frac{1}{\text{Pe}} \nabla \cdot (\lambda_\varphi \nabla T_\varphi) \quad (6)$$

where the contribution of the pressure work and heat dissipation due to viscous forces in the energy balance are neglected because the fluids are assumed to be incompressible. The volumetric heat source term was omitted in (6). This has been done for a simpler presentation and because it does not play any role in the development of the method provided that it varies periodically along the channel. Using the decomposition (3) the previous equation becomes:

$$\begin{aligned} \frac{\partial \rho_\varphi C_{p,\varphi} \Theta_\varphi}{\partial t} + \nabla \cdot \left( \rho_\varphi C_{p,\varphi} \Theta_\varphi \vec{v}_\varphi - \frac{1}{\text{Pe}} \lambda_\varphi \nabla \Theta_\varphi \right) = -\rho_\varphi C_{p,\varphi} v_\varphi \theta_\varphi + \frac{2}{\text{Pe}} \lambda_\varphi \frac{\partial \theta_\varphi}{\partial y} \\ - y \left[ \frac{\partial \rho_\varphi C_{p,\varphi} \theta_\varphi}{\partial t} + \nabla \cdot \left( \rho_\varphi C_{p,\varphi} \theta_\varphi \vec{v}_\varphi - \frac{1}{\text{Pe}} \lambda_\varphi \nabla \theta_\varphi \right) \right] \end{aligned} \quad (7)$$

where  $v_\varphi$  is the component of the velocity  $\vec{v}_\varphi$  in stream-wise direction.

In this paper, we consider incompressible fluids only. Also, we assume that the temperature variations are small and, therefore, the fluids properties can be considered as constant. Since all the quantities and the fluid properties in the equation above are periodic in  $y$  with the same periodicity length the last term in (7) has to be equal to zero:

$$\frac{\partial \rho_\varphi C_{p,\varphi} \theta_\varphi}{\partial t} + \nabla \cdot \left( \rho_\varphi C_{p,\varphi} \theta_\varphi \vec{v}_\varphi - \frac{1}{\text{Pe}} \lambda_\varphi \nabla \theta_\varphi \right) = 0 \quad \varphi = 1, 2 \quad (8)$$

This represents the advection-diffusion equation for  $\theta_\varphi$ . It depends only on the flow characteristics and there is no dependence on the reduced temperature  $\Theta_\varphi$ .

The equation for the reduced enthalpy  $C_{p,\varphi} \Theta_\varphi$  is then

$$\frac{\partial \rho_\varphi C_{p,\varphi} \Theta_\varphi}{\partial t} + \nabla \cdot \left( \rho_\varphi C_{p,\varphi} \Theta_\varphi \vec{v}_\varphi - \frac{1}{\text{Pe}} \lambda_\varphi \nabla \Theta_\varphi \right) = -\rho_\varphi C_{p,\varphi} v_\varphi \theta_\varphi + \frac{2}{\text{Pe}} \lambda_\varphi \frac{\partial \theta_\varphi}{\partial y} \quad \varphi = 1, 2 \quad (9)$$

Note that in this equation two additional terms appear. The first one ( $-\rho_\varphi C_{p,\varphi} v_\varphi \theta_\varphi$ ) represents the influence of the heat convection while the other one ( $\frac{2}{\text{Pe}} \lambda_\varphi \frac{\partial \theta_\varphi}{\partial y}$ ) takes in account the heat conduction in stream-wise direction.

## 2.1 Interface jump conditions

To describe the behavior of the new quantities at the interface, jump conditions has to be specified. For a two-phase system with reversible heat transfer at the interface the temperature is continuous over the interface (Ishii , 1975), that is:

$$T_{1i} = T_{2i} \quad (10)$$

Using the definition for the linear temperature coefficient and the fact that the flow is spatially periodic, it implies that  $\theta$  is also continuous:

$$\theta_{1i} = \theta_{2i} \quad (11)$$

Introducing the temperature decomposition (3) in (10) and using the jump relation (11) the jump condition for the reduced temperature is:

$$\Theta_{1i} = \Theta_{2i} \quad (12)$$

which means that both  $\theta$  and  $\Theta$  fields are continuous in all the computational domain, the same as the temperature.

For the heat transfer problems, a second jump condition concerning the interface heat fluxes exists. Using the Fourier law to express the heat flux, this jump condition is

$$-\lambda_1 \left. \frac{\partial T}{\partial n} \right|_{1i} + \lambda_2 \left. \frac{\partial T}{\partial n} \right|_{2i} = 0 \quad (13)$$

Since the flow is periodic it means that if  $(x_i, y_i, z_i)$  is a point on the interface separating the two fluids, the point  $(x_i, y_i + L, z_i)$  is also an interface point and the jump condition (13) applies. Thus, for the linear temperature coefficient one has:

$$\lambda_1 \left. \frac{\partial \theta_1}{\partial n} \right|_{1i} = \lambda_2 \left. \frac{\partial \theta_2}{\partial n} \right|_{2i} \quad (14)$$

The interface jump condition for the flux of the reduced temperature can be obtained introducing the decomposition (3) in (13). Using this procedure and taking in account the jump condition (14) one has:

$$\lambda_1 \left. \frac{\partial \Theta}{\partial n} \right|_{1i} + \lambda_1 \theta_{1i} \vec{e}_y \cdot \vec{n} = \lambda_2 \left. \frac{\partial \Theta}{\partial n} \right|_{2i} + \lambda_2 \theta_{2i} \vec{e}_y \cdot \vec{n} \quad (15)$$

One can see that the flux for  $\theta$  across the interface is continuous while in the case of the reduced temperature  $\Theta$  a supplementary term appears.

## 2.2 Boundary conditions

In order to have a complete system, the boundary conditions have to be specified. For stream-wise direction periodic boundary conditions for both  $\theta$  and  $\Theta$  are imposed since the heat transfer is fully developed.

For the other two directions the channel is bounded by straight walls. Using the definition for  $\theta$  and the fact that the wall heat flux is uniform one gets:

$$\begin{aligned} \lambda_1 \left. \frac{\partial \theta_1}{\partial n} \right|_{wall} &= \lambda_1 \left. \frac{\partial T_1(x, y + L, z)}{\partial n} \right|_{wall} - \lambda_1 \left. \frac{\partial T_1(x, y, z)}{\partial n} \right|_{wall} \\ &= q(x, y + L, z) - q(x, y, z) = 0 \end{aligned} \quad (16)$$

which means that the linear temperature coefficient obeys an adiabatic wall boundary condition. In the above formula it has been assumed that there is only fluid 1 near the walls (wetted walls).

For the reduced temperature, since the walls are parallel to the flow direction, one has:

$$\lambda_1 \left. \frac{\partial \Theta}{\partial n} \right|_{wall} = \lambda_1 \left. \frac{\partial T}{\partial n} \right|_{wall} - y \lambda_1 \left. \frac{\partial \theta}{\partial n} \right|_{wall} = q \quad (17)$$

where,  $n$  denotes the direction normal to the wall, i.e. either  $x$  or  $z$ . Note that the temperature  $T$  and the reduced temperature  $\Theta$  have the same wall boundary condition.

The equation (8) together with the boundary conditions (16) and the jump relations (11) and (14) indicate that for the linear temperature coefficient one has the same type of problem as for the temperature in an adiabatic flow. This implies that, for a fully developed convective heat transfer,  $\theta$  is constant both in time and space:

$$\theta_\varphi(x, y, z; t) = \theta = \text{const.} \quad (18)$$

Thus, it is not necessary to solve the partial differential equation (8). Instead,  $\theta$  can be determined directly from an algebraic equation, see subsection 2.4.

### 2.3 Volume-averaged equation for the reduced temperature

Since we use a finite volume method, we derive the governing equations by averaging the local equations over a fixed control volume  $\Omega$  (see Sabisch et al. (2001) and Ghidersa (2003) for details). The heat convection equation for the reduced enthalpy can be obtained applying the averaging operator

$$\langle \Psi \rangle = \sum_{\varphi=1,2} \frac{1}{V} \int_{\Omega} \Psi X_{\varphi}(\vec{x}, t) dV \quad (19)$$

to the local energy equation (9). In the above formula,  $X_{\varphi}$  is the characteristic function for fluid  $\varphi$  inside  $\Omega$

$$X_{\varphi}(\vec{x}, t) = \begin{cases} 1, & \vec{x} \in \Omega_{\varphi}(t), \\ 0, & \text{otherwise.} \end{cases} \quad (20)$$

where  $\Omega_{\varphi}(t)$  is the that part of the control volume that is occupied by fluid  $\varphi$  and,  $V$  is the volume of the domain  $\Omega$ . Since  $\theta$  is constant the last term in (9) vanishes and the equation is

$$\frac{\partial}{\partial t} \langle \rho C_p \Theta \rangle + \nabla \cdot \left( \langle \rho C_p \Theta \vec{v} \rangle - \frac{1}{\text{Pe}} \langle \lambda \nabla \Theta \rangle \right) = - \langle \rho C_p v \rangle \theta - \frac{1}{\text{Pe}} (\lambda_1 - \lambda_2) \theta \frac{1}{V} \int_{S_i} \vec{e}_y \cdot \vec{n} dS \quad (21)$$

The last term in (21) appears because of the interface heat flux jump condition (15).

### 2.4 Linear temperature coefficient

To find the value of  $\theta$  one can use the equation (21) where  $\Omega$  is taken to be the entire computational domain  $[0, L_x] \times [0, L] \times [0, L_z]$ :

$$\begin{aligned} \frac{\partial}{\partial t} \sum_{\varphi=1,2} \int_{\Omega} \rho_{\varphi} C_{p,\varphi} \Theta_{\varphi} X_{\varphi} dV + \sum_{\varphi=1,2} \left( \int_{S_L} \rho_{\varphi} C_{p,\varphi} \Theta_{\varphi} v_{\varphi} X_{\varphi} dS - \int_{S_0} \rho_{\varphi} C_{p,\varphi} \Theta_{\varphi} v_{\varphi} X_{\varphi} dS \right) \\ - \frac{1}{\text{Pe}} \sum_{\varphi=1,2} \left( \int_{S_L} \lambda_{\varphi} \frac{\partial \Theta_{\varphi}}{\partial y} X_{\varphi} dS - \int_{S_0} \lambda_{\varphi} \frac{\partial \Theta_{\varphi}}{\partial y} X_{\varphi} dS \right) \\ = \frac{1}{\text{Pe}} \frac{Q}{L} - \theta \sum_{\varphi=1,2} \int_V \rho_{\varphi} C_{p,\varphi} v_{\varphi} X_{\varphi} dV - \theta (\lambda_1 - \lambda_2) \int_{S_i} \vec{e}_y \cdot \vec{n} dS \quad (22) \end{aligned}$$

where  $S_0$  and  $S_L$  designate the inflow and, respectively, the outflow cross sections,  $V$  is the volume of  $\Omega$ , and  $S_i$  is the interface separating the two fluids.  $Q$  is the rate of heat addition through the channel walls defined as

$$Q = \frac{2(L_x + L_z)}{L_x L_z} q \quad (23)$$

Since the heat transfer is fully developed and all the quantities are periodic in stream-wise direction all the terms on the l.h.s. of equation (22) are zero. Also,  $S_i$  can be considered as a closed surface since the bubbles along the channels have the same shape. This means that the last term in the equation is equal to zero. Thus, for  $\theta$  one has

$$\theta = \frac{1}{\text{Pe}} \frac{Q}{L \sum_{\varphi=1,2} \int_V \rho_{\varphi} C_{p,\varphi} v_{\varphi} X_{\varphi} dV} \quad (24)$$

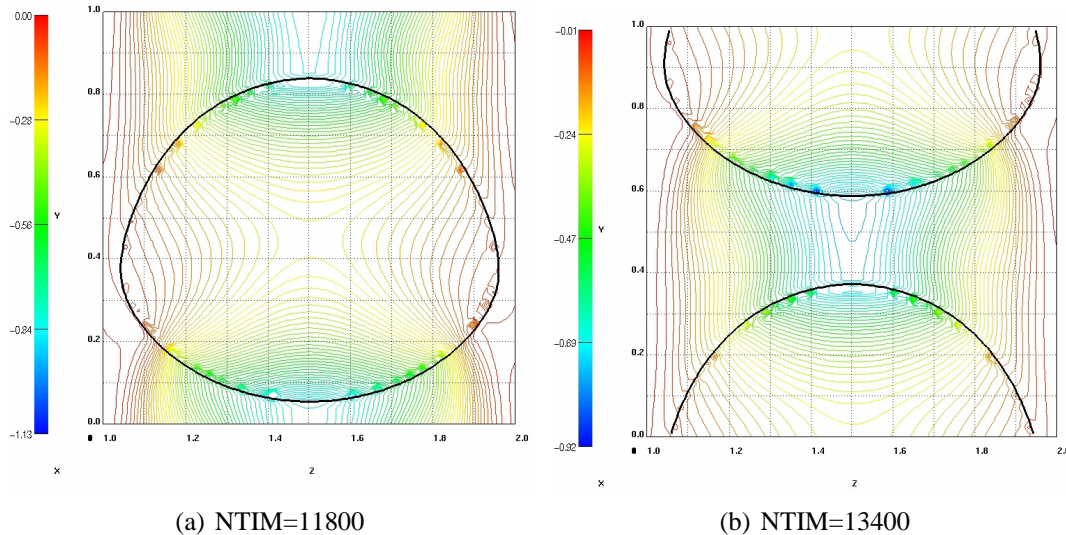


Figure 1: Temperature field in a longitudinal plane containing the channel axis for two different instants in time.

## 2.5 Numerical method

To approximate numerically the equation (21) a finite volume procedure is used. In order to reduce the oscillations of the solution near the interface the convective fluxes are constructed using an upwind scheme. While a central differences approach would be stable only for  $Pe$  numbers smaller than 2, the upwind approximation is not limited by this parameter. For the conductive term, the heat fluxes at the cell faces are approximated using a formula proposed by Patankar et al. (1977). This formula computes the heat flux through a certain face of the cell exactly in the case when the interface between the fluids and that face are coincidental. When the interface is cutting the cell the heat flux is approximated assuming that each cell is filled with a fluid with the same properties as the mixture from that cell. The time integration is done using an explicit third order Runge-Kutta scheme. Further details on the numerical method can be found in Ghidersa (2003).

## 3 Results and discussions

This section presents the results of a simulation using the model introduced in section 2 as implemented in our computer code TURBIT-VOF (Ghidersa, 2003) for the flow of a train of large bubbles uniformly distributed along a 2 mm wide channel with square cross-section. The channel is vertical and the fluids are moving co-currently in upward direction. The computational domain is a cube of size 2 mm and the non-dimensional size is  $1 \times 1 \times 1$ . This box is discretized by  $64 \times 64 \times 64$  uniform mesh cells. At the four side walls of the square channel a uniform heat flux is imposed while in stream-wise direction the presence and influence of the neighboring unit cells is simulated by periodic boundary conditions.

For this numerical simulation we take a density ratio of  $\rho_2/\rho_1 = 0.013$ , a viscosity ratio of  $\mu_2/\mu_1 = 0.04$ , a specific heat capacity ratio of  $C_{p,2}/C_{p,1} = 0.2401$  and a thermal conductivity ratio of  $\lambda_2/\lambda_1 = 0.0451$ . The Prandtl number for the liquid is  $Pr = 2.34$  which means that for the gas one has  $Pr = 0.5$ .

The simulation is started with gas and liquid at rest and a constant pressure drop in stream-wise direction is imposed. Initially, the temperature in the channel is assumed to be uniform. The flow is considered to be fully developed, both hydrodynamic and thermal, when the superficial velocity becomes constant and the mean temperature in the computational domain is stationary.

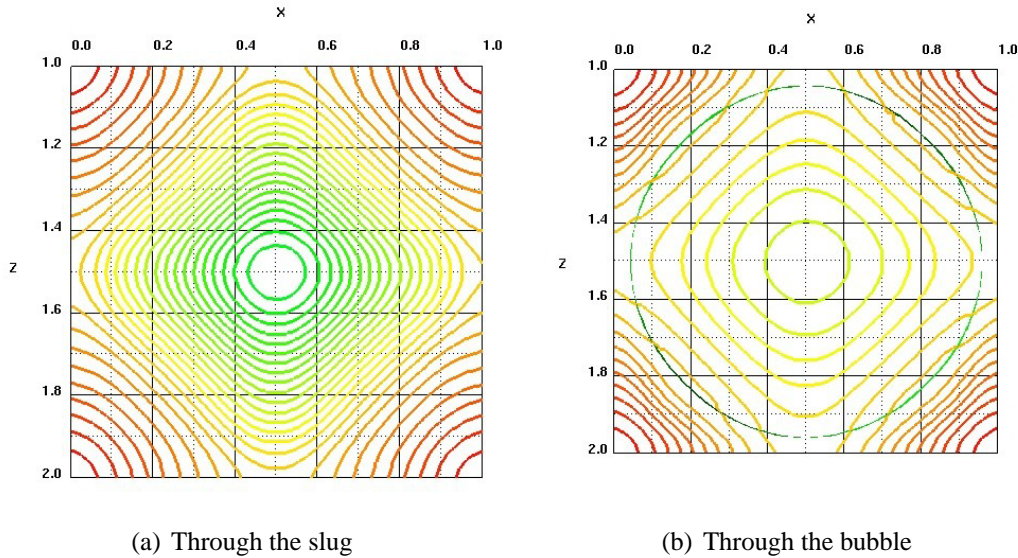


Figure 2: Isolines of the temperature field in a transversal plane at  $NTIM=11400$ .

In this paper we present only the results concerning the heat transfer. A detailed analysis of the flow structure, bubble shape and film thickness can be found in Ghidersa (2003) and Ghidersa et al. (2004). In Figure 1 the structure of the temperature field inside the bubble and in the liquid slug is visualized. The presence of the gas in the channel modifies the temperature field as compared to single phase heat convection. The isothermal lines show that gas has higher temperature in the region where the bubble interface is closer to the walls. However, moving towards the center of the channel the temperature decreases slower in the bubble than it does in the liquid phase. Since the heat conductivity of the gas is lower than the one corresponding to the liquid the only explanation for this behavior is the strong recirculation inside the bubble which transports the hotter gas near the interface towards the center of the bubble. For the liquid slug this mixing effect is smaller and there is a region in the center of the channel where the liquid remains colder. This can be observed also comparing the temperature field in two cross-sections, one through the liquid slug (Fig. 2(a)) and the other at the position, along the channel, where the bubble has the largest diameter (Fig. 2(b)). In these figures the temperature isolines are represented using the same number of iso-levels between the maximum and the minimum temperature. These limits are computed for the whole domain therefore one can directly correlate the magnitude of the temperature gradient with the density of the isolines. Thus, in the slug one can identify a region with large temperature gradients making the transition from the higher temperature in the corners of the channel to the lower temperature in the central region. In the cross-sections where the bubble is present the temperature gradients are larger in the liquid layer surrounding the interface at the corners of the channel. Inside the bubble the gradient is much smaller because of the heat convection due to inner recirculation.

An other interesting aspect about the transverse temperature distribution is the direction of the temperature gradients. For the single phase heat convection problem, when the flow is laminar, the heat transfer is done only by conduction in the direction perpendicular to the wall. The temperature isolines are, in this case, concentric circles and the temperature gradient points toward the center of the channel. For the bubble train flow, the isolines pattern changes. Because of the lateral movement of the liquid induced by the passage of the bubbles, a part of the heat from the middle of the wall is transported towards the channel corners. In the liquid slug (see Fig. 2(a)), looking along a diagonal, the isolines are first concentric arcs with the center in the corner of the channel. Moving towards the center of the channel, there is a region where the temperature is constant in the direction perpendicular

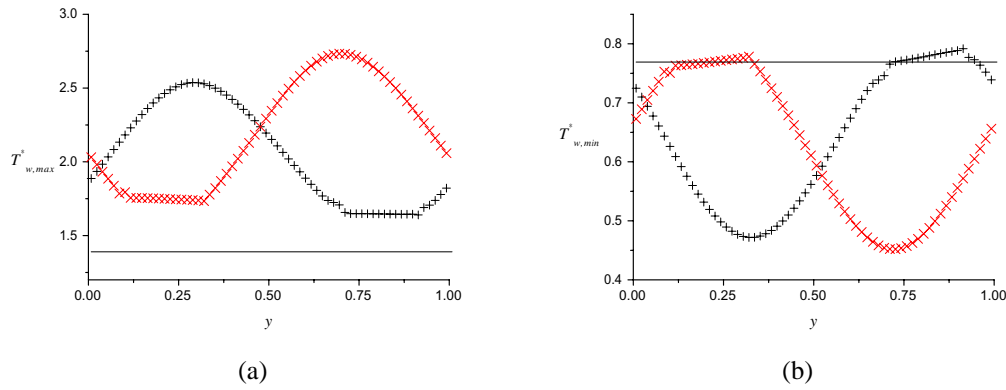


Figure 3: Normalized maximum and minimum wall temperature variation along the channel for two different time-steps: (+): NTIM=11400; (x): NTIM=12600; continuous line: single phase flow.

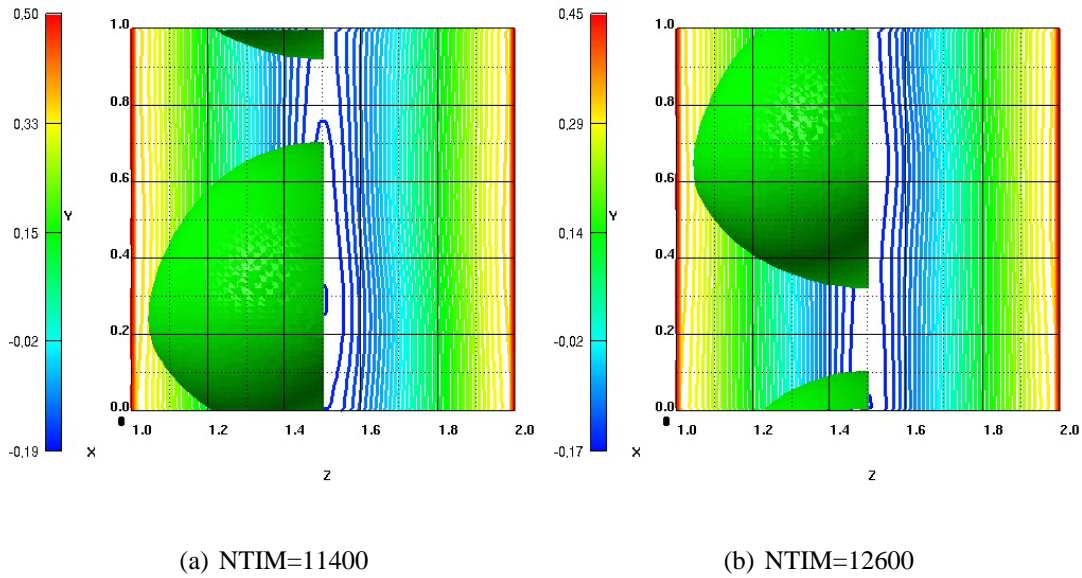


Figure 4: Wall temperature ( $T_w$ ) isolines at two different time steps.

to the diagonal while, close to the center the isolines form concentric circles. The same picture holds in a cross-section through the bubble, the isolines being slightly deformed due to the presence of the interface (see Fig. 2(b)). This pattern suggests that, compared to the single phase situation, the heat transfer improves in the middle part of the wall while it diminishes in the corners of the channel. This observation is confirmed by comparing the normalized maximum and minimum wall temperatures given by

$$T_{w,max}^* = \frac{T_{w,max} - T_c}{T_{w,m} - T_c} \quad (25)$$

$$T_{w,min}^* = \frac{T_{w,min} - T_c}{T_{w,m} - T_c} \quad (26)$$

with the corresponding values for the single phase flow. In the formulas above  $T_c$  is the temperature on the center line of the channel,  $T_{w,m}$  is the mean temperature at the wall and,  $T_{w,max}$ ,  $T_{w,min}$  are the maximum and, respectively, minimum temperature at the wall. In Figure 3 the variation along the channel for  $T_{w,max}^*$  (Fig. 3(a)) and  $T_{w,min}^*$  (Fig. 3(b)) are presented. Two different time steps are



considered: one (NTIM=11400) corresponding to the moment when the mixture temperature of the unit cell is close to its maximum value and the other one (NTIM=12600) close to its minimum value. The values of  $T_{w,max}^*$  and  $T_{w,min}^*$  for the single phase are represented with continuous line. From this figures one can see that the normalized maximum wall temperature, which corresponds to the temperature in the corner, is always larger in the case of bubble-train flow than when the single phase flow is considered. For the normalized minimum wall temperature, corresponding to the temperature in the middle of the wall, the values for bubbly flow are relatively close to the single phase value in the region of the liquid slug and smaller in other parts of the computational domain. For easy reference the position of the bubble and temperature isolines at the wall are given in Figure 4.

## 4 Conclusion

For spatially periodic two-phase flows in small channels a new concept to model convective heat transfer, called *periodic fully developed flow*, has been introduced. Based on the periodical characteristics of the flow, the velocity field analysis can be confined to a single isolated module. A similar analysis is done for the temperature field, but the periodicity conditions are of a different nature. For axial uniform wall heat flux the temperature itself is periodic, provided that a linear term related to the bulk enthalpy change is subtracted.

Using this method, the bubble-train flow along a square channel with uniform wall heat flux has been simulated. Both axial, and transverse temperature variation could be analyzed, and the changes due to the presence of the gas bubble could be studied. Thus, in the liquid, an improvement of the heat transfer in the middle of the channel faces could be observed due to the liquid movements toward the channel corners where a decrease of the heat transfer characteristics could be seen. Inside the gas bubbles the strong mixing has the tendency to reduce temperature gradients.

These results show that this new method is a valuable tool for the numerical analysis of spatially periodic two-phase flows in channels with heat transfer. Using global quantities as input parameters the method allows the reconstruction of the local flow or temperature field. For low mass fluxes the temperature-mass analogy can be also used to compute the local concentrations of different species in the channel. Here it is referred to the chemical substances that are passively transported by the flow. When chemical reactions take place and new products are generated an extension of the actual version of the code has to be done in order to account for these phenomena.

This numerical method is, however, restricted to spatially periodic flows only. This limitation is quite severe when heat transfer is concerned. When phenomena like phase change at the interface or exothermal reactions between reactants transported by the flow occur, the heat exchange depends strongly on local temperature and can not be regarded as periodic anymore. To extend the applicability of the code for more general cases the introduction of inflow and outflow boundary conditions is mandatory to replace the periodic boundary conditions.

The absence of experiments from the literature, that could be used to validate the results for heat transfer, represents, also, a sensible point of this work. Therefore, future experiments to verify the numerical results measurements of wall temperature or temperature profiles inside the channel should be performed.

## Nomenclature

$C_p$	specific heat
$\vec{e}_y$	unit vector in stream-wise direction
$L$	periodicity length
$\vec{n}$	normal vector to the interface
Pe	Peclet number

$Q$	rate of the heat addition through channel walls
$q$	wall heat flux
$Re$	Reynolds number
$S_i$	interfacial area
$T$	temperature
$t$	time
$\vec{v}$	velocity field
$V$	volume of the control domain
$v$	stream-wise component of the velocity
$X$	characteristic function for each fluid (phase)
$x, y, z$	Cartesian co-ordinates

#### *Greek symbols*

$\lambda$	heat conductivity
$\Omega$	control domain
$\Theta$	reduced temperature
$\theta$	linear temperature coefficient
$\rho$	density

#### *Subscripts*

$\varphi$	associated to phase $\varphi$
$\varphi^i$	value at the interface associated to phase $\varphi$

## **References**

- Ehrfeld, W., Hessel, V., Löwe, H., 2000. *Microreactors: New technology for modern chemistry*, Wiley-VCH, Weinheim.
- Ghidersa, B.E., 2003. Finite Volume-based Volume-of-Fluid method for the simulation of two-phase flows in small rectangular channels. Ph.D. thesis, Universität Karlsruhe (TH), <http://www.ubka.uni-karlsruhe.de/cgi-bin/psview?document=2003/maschinenbau/10>.
- Ghidersa, B.E., Wörner, M., Cacuci, D.G., 2004. Exploring the flow of immiscible fluids in a square vertical mini-channel by direct numerical simulation. *Chem. Eng. J.*, *accepted for publication*.
- Haverkamp, V., Emig, G., Hessel, V., Liauw, M.A., Löwe, H., 2002. Characterization of a Gas/Liquid Microreactor, the Micro Bubble Column: determination of Specific Interfacial Area, in M. Matlosz, W. Ehrfeld, J.P. Baselt (Eds.): *Microreaction Technology, IMRET-5: Proc. Fifth Int. Conf. on Microreaction Technology*, Springer, 203–214.
- Ishii, M., 1975, *Thermo–fluid dynamic theory of two–phase flow*. Eyrolles, Paris.
- Jensen, K.F., 2001. Microreaction engineering - is small better? *Chem. Eng. Sci.* 56, 293–303.
- Jongen, N., Donnet, M., Bowen, P., Lemaître, J., Hofmann, H., Schenk, R., Hofmann, C., Aoun-Habbache, M., Guillement-Fritsch, S., Sarria, J., Rousset, A., Viviani, M., Buscaglia, M.T., Buscaglia, V., Nanni, P., Testino, A., Herguijuela, J.R., 2003. Development of a Continuous Segmented Flow Tubular Reactor and the "Scale-out" Concept - In Search of Perfect Powders. *Chem. Eng. Technol.* 26, 303–305.

- Patankar, S.V., Liu, C.H., Sparrow, E.M., 1977. Fully developed flow and heat transfer in ducts having stream-wise-periodic variations of cross-sectional area. *Journal of Heat Transfer* 99 , 180–186.
- Sabisch, W., Wörner, M., Grötzbach, G., Cacuci, D.G., 2001. 3D volume-of-fluid simulation of a wobbling bubble in a gas-liquid system of low Morton number. *Fourth International Conference on Multiphase Flow, ICMF-2001, New-Orleans, Louisiana, U.S.A., May 27 - June 1*, paper 244.
- Schubert, K., Brandner, J., Fichtner, M., Linder, G., Schygulla, U., Wenka, A., 2001. Microstructure devices for applications in thermal and chemical engineering. *Microscale Thermophysical Engineering* 5, 17–39.
- Thulasidas, T.C., Abraham, M.A., Cerro, R.L., 1995. Bubble-train flow in capillaries of circular and square cross section. *Chem. Eng. Sci.* 50, 183–199.
- Thulasidas, T.C., Abraham, M.A., Cerro, R.L., 1999. Dispersion during bubble-train flow in capillaries. *Chem. Eng. Sci.* 54, 61–67.